Complex-temperature properties of the two-dimensional Ising model for nonzero magnetic field

Victor Matveev* and Robert Shrock†
Institute for Theoretical Physics, State University of New York, Stony Brook, New York 11794-3840
(Received 10 July 1995)

We study the complex-temperature phase diagram of the square-lattice Ising model for nonzero external magnetic field H, i.e., for $0 \le \mu \le \infty$, where $\mu = e^{-2\beta H}$. We also carry out a similar analysis for $-\infty \le \mu \le 0$. The results for the interval $-1 \le \mu \le 1$ provide a way of continuously connecting the two known exact solutions of this model, viz., at $\mu = 1$ (Onsager, Yang) and $\mu = -1$ (Lee and Yang). Our methods include numerical calculations of complex-temperature zeros of the partition function and an analysis of low-temperature series expansions. For real nonzero H, the inner branch of a limaçon bounding the FM phase breaks and forms two complex-conjugate arcs. We study the singularities and associated exponents of thermodynamic functions at the endpoints of these arcs. For $\mu < 0$, there are two line segments of singularities on the negative and positive u axis, and we carry out a similar study of the behavior at the inner end points of these arcs, which constitute the nearest singularities to the origin in this case. Finally, we also determine the exact complex-temperature phase diagrams at $\mu = -1$ on the honeycomb and triangular lattices and discuss the relation between these and the corresponding zero-field phase diagrams.

PACS number(s): 05.50.+q

I. INTRODUCTION

The two-dimensional Ising model serves as a prototype of a statistical mechanical system that undergoes a phase transition with associated spontaneous symmetry breaking and long-range order. The free energy of the (spin-$\frac{1}{2}$) Ising model was first calculated by Onsager [1], and the expression for the spontaneous magnetization first derived by Yang [2] (both for the square lattice). However, the model has never been solved in an arbitrary nonzero external magnetic field, and this has long remained an outstanding open problem. Hence, any additional information that one can gain about the Ising model in a magnetic field is of value. In elucidating the properties of the zero-field model, it has proved useful to generalize the temperature variable to complex values. There are several reasons for this. First, one can understand more deeply the physical behavior of various thermodynamic quantities by seeing how they vary as analytic functions of complex temperature (CT). Second, one can see how the physical phases of a given model generalize to regions in appropriate complex-temperature variables. Third, a knowledge of the complex-temperature singularities of quantities that have not been calculated exactly helps in the search for exact, closed-form expressions for these quantities. For the (spin-$\frac{1}{2}$) zero-field Ising model on the square lattice the complex-temperature zeros of the partition function were first discussed in Refs. [3, 4] and the associated phase diagram is known exactly. In the complex Boltzmann weight variable $z = e^{-2K}$ (see below for notation) the phase boundaries consist of two intersecting circles with a $z \to -z$ symmetry; more compactly, in the variable $u = z^2$, which incorporates this symmetry, they are given by a limaçon of Pascal [5]. Just as this generalization to complex temperature has yielded a deeper insight into the zero-field model, so also can it shed light on the behavior of the model for nonzero field. Accordingly, in this paper, we shall investigate the complex-temperature properties of the two-dimensional (2D) Ising model for nonzero external field. Our methods include calculations of complex-temperature zeros of the partition function and analyses of low-temperature series expansions.

Although no one has solved the 2D Ising model in an arbitrary field, Lee and Yang did succeed in solving exactly for the free energy and magnetization for a particular manifold of values of H depending on the temperature T, given by $H = i(\pi/2)k_BT$ [6] (see also [7]). Although this is not a physical set of values, owing to the imaginary value of H and the resultant nonhermiticity of the Hamiltonian, this model is nevertheless of considerable interest for the insight that it yields into the properties of the Ising model in the presence of a symmetry-breaking field. By an extension of our analysis to complex values of H, we are able to continuously connect the two known exact solutions of the 2D Ising model, at $H = 0$ [1, 2] and at $H = i(\pi/2)k_BT$ [6].

Before proceeding, we mention some related work. Rigorous results on the behavior of the model for nonzero external field H include the theorem that, for ferromagnetic (FM) spin-spin coupling, $J > 0$, the free energy $F(T, H)$ is an analytic function of temperature [7, 8]. In the case of antiferromagnetic (AFM) coupling, $J < 0$, this is not the case; there is a temperature $T_b(H)$ such that as T decreases through $T_b(H)$, the system under-

*Electronic address: vmatveev@max.physics.sunysb.edu
†Electronic address: shrock@max.physics.sunysb.edu

goes a (first-order) transition from FM to AFM long-range order. Although there is no known exact expression for $T_b(H)$, accurate numerical values are known (e.g., [9] and references therein). In addition to the works noted above [3,4], papers on complex-temperature singularities in the 2D square-lattice Ising model for $H = 0$ include Refs. [12–16]. A useful connection between the Lee-Yang solution for $\beta H = i\pi/2$ and a modified zero-field Ising model with certain coupling(s) shifted by $i\pi/2$ was discussed in Refs. [17, 18]. The complex-temperature phase diagram for the Lee-Yang case $\beta H = i\pi/2$ was worked out in Ref. [19], inlcuding exact results for the specific heat and magnetization critical exponents and series analyses to determine the susceptibility critical exponents at certain complex-temperature singularities. Complex-temperature zeros of the partition were studied for the 3D Ising model in a nonzero magnetic field in Ref. [20]. In contrast to the Ising model, a certain superexchange model can be solved exactly in a field [21]. We have studied the complex-temperature properties of this model for nonzero field and will report the results elsewhere. Whereas here we study complex-temperature zeros of the partition function for real and certain complex values of magnetic field, a different complexification is to study the zeros of Z in the complex magnetic field for physical temperature [7, 6]. This led to the famous theorem [7,6] that for ferromagnetic couplings the zeros in the complex $e^{-2\beta H}$ plane lie on a circle and pinch the positive real axis as the temperature decreases through its critical value; this work also derived integral relations expressing thermodynamic quantities in terms of integrals of densities of complex-field zeros. Similar relations for complex-temperature zeros were later discussed in Refs. [3, 10].

II. GENERAL PROPERTIES

A. Model

Our notation is standard and follows that in our earlier works (e.g., [5, 19]), so we review it only briefly. The (spin-$\frac{1}{2}$, isotropic, nearest-neighbor) Ising model on the square lattice is defined by the partition function

$$Z = \sum_{\{\sigma_n\}} e^{-\beta \mathcal{H}}, \tag{2.1}$$

with the Hamiltonian

$$\mathcal{H} = -J \sum_{\langle nn' \rangle} \sigma_n \sigma_{n'} - H \sum_n \sigma_n, \tag{2.2}$$

where $\sigma_n = \pm 1$ are the Z_2 spin variables on each site n of the lattice, $\beta = (k_B T)^{-1}$, J is the exchange constant, $\langle nn' \rangle$ denotes nearest-neighbor sites, and the units are defined such that the magnetic moment that would multiply the $H \sum_n \sigma_n$ is unity. (Hereafter, we shall use the term "Ising model" to denote this model unless otherwise indicated.) For $H = 0$, the symmetry group of the theory is Z_2. We use the notation

$$K = \beta J \ , \quad h = \beta H, \tag{2.3}$$

$$z = e^{-2K} \ , \quad u = z^2 = e^{-4K} \ , \quad v = \tanh K \tag{2.4}$$

and

$$\mu = e^{-2h}. \tag{2.5}$$

The reduced free energy per site is $f = -\beta F = \lim_{N_s \to \infty} N_s^{-1} \ln Z$ in the thermodynamic limit, where N_s is the number of sites on the lattice. The zero-field susceptibility is $\chi = \frac{\partial M(H)}{\partial H}|_{H=0}$, where $M(H)$ denotes the magnetization. It is convenient to deal with the reduced quantity $\bar{\chi} = \beta^{-1}\chi$.

A useful property is that the partition function Z is a generalized polynomial (with both negative and positive integral powers) in u and μ. (For a lattice with odd coordination number, Z would be a generalized polynomial in z and μ.) On a finite lattice, for fixed μ, Z thus has a certain set of zeros in the u plane. Experience with the zero-field model shows that in the thermodynamic limit, these merge together to form curves (including possible line segments) across which the free energy is nonanalytic. These are the only singularities of f, except for the trivial singularities when $|K| = \infty$ (which are isolated singularities and thus are not important for the discussion of phase boundaries). Hence, the calculation of zeros of the partition function on finite lattices serves as a valuable means by which to gain information about the above continuous locus of points where the free energy is non-analytic in the thermodynamic limit [30]. This continuous locus of points includes the phase boundaries of the complex-temperature phase diagram. It may also include certain arcs or line segments that protrude into and terminate in the interior of some phases and hence do not separate any phases.

B. Symmetries

We record here some basic symmetries that will be used in our work. First, because Z is a generalized polynomial in μ, in the analysis of the phase diagram, it suffices, with no loss of generality, to consider only the range

$$-\frac{i\pi}{2} < \mathrm{Im}(h) \le \frac{i\pi}{2}. \tag{2.6}$$

Second, the summand of the partition function is invariant under the transformation $h \to -h$, $\sigma_n \to -\sigma_n$. The sign flip $h \to -h$ is equivalent to the inversion map

$$\mu \to \frac{1}{\mu}. \tag{2.7}$$

Hence, in considering nonzero real h, one may, with no loss of generality, restrict to $h \ge 0$. More generally, in considering complex h, one may, with no loss of generality, restrict to the unit disk

$$|\mu| \leq 1 \tag{2.8}$$

in the μ plane. We shall concentrate here on the range of μ values that connect the Onsager and Lee-Yang solutions of the model, viz.,

$$-1 \leq \mu \leq 1. \tag{2.9}$$

By the above symmetry, these values suffice to describe the entire real line

$$-\infty \leq \mu \leq \infty. \tag{2.10}$$

Third, concerning the symmetries of the locus of points across which the free energy is nonanalytic and the associated complex-temperature phase diagram (and, for finite lattices, the set of zeros of Z), these are invariant under $u \to u^*$, i.e., under reflection about the horizontal, Re(u) axis. Fourth, if and only if $\mu = \pm 1$, this locus of points is invariant under the inversion map

$$u \to \frac{1}{u}. \tag{2.11}$$

This symmetry holds because of the bipartite nature of the square lattice, and this mapping interchanges the uniform and staggered magnetizations. Thus, if one starts at a point in the FM phase, the mapping takes one to a corresponding point in the AFM phase. Since, in general, the FM phase occupies a region in the neighborhood of the origin in the u (or z) plane, this shows that the AFM phase will be the outermost phase, extending to complex infinity in these two respective planes. This result is obvious for $h = 0$ and can be seen easily for the case $\mu = -1$ from the relation [17, 18] connecting this theory to a zero-field Ising model with certain couplings shifted by $i\pi/2$, as discussed in [19]. Although this inversion symmetry does not hold for $\mu \neq \pm 1$, one can still make the following statement. Let us write u in polar form, $u = \rho_u e^{i\theta_u}$. Then

$$K = -\frac{1}{4}\ln u = -\frac{1}{4}\Big(\ln \rho_u + i\theta_u + 2\pi i n\Big), \tag{2.12}$$

where n indexes the Riemann sheet of the logarithm and will not be important here (we take it to be $n = 0$). The usual limit of infinitely strong antiferromagnetic spin-spin exchange coupling $K = \beta J \to -\infty$ corresponds to u going to infinity along the positive real axis. However, Eq. (2.12) shows that as $|u| \to \infty$ along any direction, not necessarily $\theta_u = 0$, K corresponds to an infinitely strong AFM coupling, since the term $-(1/4)i\theta_u$ is finite and becomes negligible in this limit. It follows that for arbitrary fixed μ, if an AFM phase exists at all (it is absent, e.g., for the isotropic Ising model on the triangular and Kagomé lattices), then it extends outward in all directions to complex infinity in the u or z plane. This general property was evident in our earlier studies of the complex-temperature phase diagrams for the zero-field Ising model on the square, triangular, and honeycomb lattices [5, 24], as well as the heteropolygonal 3×12^2 and 4×8^2 lattices [23].

Finally, we can show a close connection between the properties of the theory in the vicinity of the origin in the μ plane by a similar argument. Small negative μ, i.e., $\mu \to 0^-$, is equivalent to small positive μ, $\mu \to 0^+$, which, in turn, corresponds to infinitely strong external field, $h \to \infty$. These results are easily seen as follows. Let us write $\mu = \rho_\mu e^{i\theta_\mu}$. Then from the definition $\mu = e^{-2h}$,

$$h = -\frac{1}{2}\ln \mu = -\frac{1}{2}\Big(\ln \rho_\mu + i\theta_\mu + 2\pi i n\Big). \tag{2.13}$$

As $\rho_\mu \to 0$, $h \to \infty$. In this limit, the term involving the argument θ_μ has a negligible effect. (This actually yields a stronger result than we need here, viz., that as $\rho_\mu \to 0$ along any direction, not just $\theta_\mu = 0$ or π, this direction becomes asymptotically unimportant, and the effect is like a physical uniform field.) This implies that in the limit as $\mu \to 0$ (along any direction), the complex-temperature phase diagram in the u plane consists only of the FM phase, with the AFM phase frozen out. As a consequence of the $h \to -h$, $\mu \to 1/\mu$ symmetry mentioned above, this also applies (with $M \to -M$) to the limit $|\mu| \to \infty$ along any direction.

III. COMPLEX-TEMPERATURE PROPERTIES FOR SOLVED CASES

A. $h = 0$ ($\mu = 1$)

In order to achieve a better understanding of the results that we shall obtain concerning the complex-temperature phase diagram for the interval $-1 < \mu < 1$ (or equivalently, the union $\{-\infty \leq \mu < -1\} \bigcup \{1 < \mu \leq \infty\}$) where the model has not been solved exactly, it is useful to discuss this phase diagram for the two cases where it is known precisely, viz., $\mu = \pm 1$. As part of Fig. 1, we show the complex-temperature phase diagram for

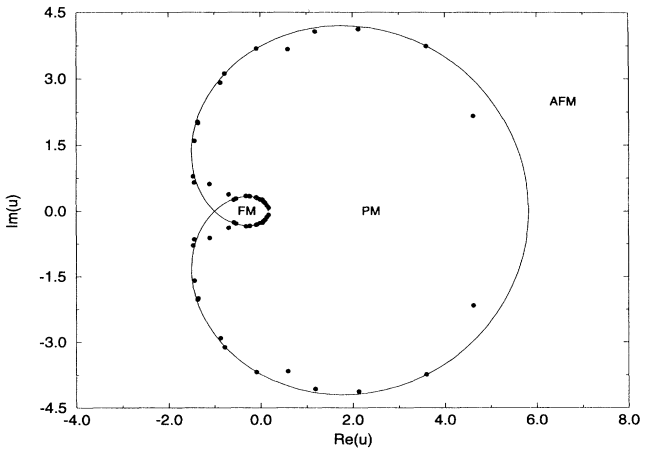

FIG. 1. Complex-temperature zeros of Z, calculated for $h = 0$ ($\mu = 1$) on a 7×8 lattice with helical boundary conditions, as compared with the exact result, in the $u = e^{-4K}$ plane.

$H = 0$ ($\mu = 1$). The phase boundaries in the u plane form a limaçon [5], given by

$$\mathrm{Re}(u) = 1 + 2^{3/2}\cos\omega + 2\cos 2\omega, \tag{3.1}$$

$$\mathrm{Im}(u) = 2^{3/2}\sin\omega + 2\sin 2\omega \tag{3.2}$$

traced out completely for $0 \le \omega < 2\pi$ (see Fig. 1). The complex-temperature extensions of the physical phases with spontaneous Z_2 symmetry breaking via ferromagnetic and antiferromagnetic long-range order lie, respectively, within the inner branch of the limaçon and outside the outer branch of this limaçon. The complex-temperature extension of the Z_2-symmetric, paramagnetic (PM) phase lies between the inner and outer branches of the limaçon. Note that the FM, AFM and (two wedges of the) PM phase are all contiguous at the point $u = -1 \equiv u_s$. Recall that the physical critical point separating the PM and FM phases is $u_c = 3 - 2\sqrt{2} = 0.171\,573...$, and, in accordance with the $u \to 1/u$ symmetry noted above, the corresponding critical point separating the PM and AFM phase is $u = 1/u_c = 3 + 2\sqrt{2} = 5.828\,43...$. Henceforth, we shall generally refer to these phases simply as FM, AFM, and PM, with the qualifier "complex-temperature extension" being understood. The corresponding phase boundaries in the z plane consist of the intersecting circles $z = \pm 1 + 2^{1/2}e^{i\theta}$, $0 \le \theta < 2\pi$ [3,4]. (In this variable, there are actually four phases: FM, AFM, PM, and O, where the O phase has no overlap with any physical phase [5].)

The spontaneous magnetization is

$$M(u, h = 0) = \frac{(1+u)^{1/4}[(1-u/u_c)(1-u_c u)]^{1/8}}{(1-u)^{1/2}} \tag{3.3}$$

in the physical FM phase [2], and this expression holds, by analytic continuation, throughout the complex-temperature extension of the FM phase ($M = 0$ elsewhere). Thus, M vanishes continuously both at the physical critical point $u = u_c$ and at the point $u = -1 \equiv u_s$. M vanishes discontinuously elsewhere along the boundary of the (complex-temperature extension of the) FM phase. As discussed in Ref. [5], the apparent singularities at $u = 1/u_c$ and $u = 1$ do not actually occur since these points lie outside the FM phase where the above expression applies; indeed, M vanishes identically in the vicinity of $u = 1/u_c$ and $u = 1$. By a well-known symmetry, the staggered magnetization is given by $M_{st}(y) = M(u \to y)$, where $y = 1/u$, in the AFM phase and is zero elsewhere. In addition to its well-known divergence at the physical critical point, the susceptibility $\bar{\chi}$ diverges at $u = -1$ with exponent inferred from series analysis to be $\gamma_s' = 3/2$ [5, 16]. Reference [5] obtained the relation

$$\gamma_s = 2(\gamma - 1), \tag{3.4}$$

which explains the value of γ_s' in terms of that of the usual exponent $\gamma = 7/4$.

B. $h = i\pi/2$ ($\mu = -1$)

In Ref. [19] we determined the locus of points across which the free energy is nonanalytic, and the corresponding complex-temperature phase diagram, for the Lee-Yang solution at $\mu = -1$. These consist of the union of the unit circle and a certain line segment on the negative real u axis:

$$\{\, u = e^{i\theta}\ ,\ \theta \in [0, 2\pi)\,\} \bigcup \{\, 1/u_e \le u \le u_e\,\}, \tag{3.5}$$

where

$$u_e = -(3 - 2\sqrt{2}) \tag{3.6}$$

(which is also equal to minus the value of the critical point u_c in the $h = 0$ model). Since the nonzero value of H explicitly breaks the Z_2 symmetry, there is no PM phase. The FM and AFM phases occupy the interior and exterior of the unit circle, respectively. In contrast to the $h = 0$ case, here a subset of the continuous locus of points across which f is nonanalytic, viz., the line segment in (3.5), does not completely separate any phases, but instead protrudes into the FM and AFM phases, terminating in the respective end points $u = u_e$ and $u = 1/u_e$. The magnetization is [6]

$$M(u, h = i\pi/2) = \frac{(1+u)^{1/2}}{(1-u)^{1/4}[(1-u/u_e)(1-u_e u)]^{1/8}} \tag{3.7}$$

within the FM phase (and zero elsewhere). As is clear from (3.7), this vanishes continuously at $u = -1$ with exponent $\beta_s = 1/2$, and diverges at $u = u_e$ with exponent $\beta_e = -1/8$ and at $u = 1$ with exponent $\beta_1 = -1/4$. Elsewhere on the boundary of the FM phase, i.e., the unit circle in the u plane, M vanishes discontinously. Note that the apparent divergence at the point $u = 1/u_e$ does not actually occur, since this is outside of the complex-temperature FM phase, where the above analytic continuation is valid. From analyses of low-temperature series, we concluded that $\bar{\chi}$ has divergent singularities (i) at $u = u_e$ with exponent $\gamma_e' = 5/4$, (ii) at $u = 1$, with exponent $\gamma_1' = 5/2$, and (iii) at $u = u_s = -1$, with exponent $\gamma_s' = 1$ [19]. (The actual values obtained from series analysis were $\gamma_e' = 1.25 \pm 0.01$, $\gamma_1' = 2.50 \pm 0.01$, and $\gamma_s' = 1.00 \pm 0.08$.)

C. Partition function zeros for solved cases

1. $\mu = 1$

Since one of our two main methods of gaining information about the complex-temperature phase diagram of the model for $\mu \ne \pm 1$ is the use of complex-temperature zeros of Z, it is important to see how accurate this

method is for the two cases where one knows the phase diagram exactly, viz., $\mu = \pm 1$. That is, we wish to ascertain how well, for finite lattices with various boundary conditions, the pattern of zeros resembles the locus of points across which f is nonanalytic in the thermodynamic limit.

In order to compute the zeros, we calculate Z for finite lattices with specified boundary conditions (BC's). We have done this by means of a transfer matrix method [25], and have used both periodic and helical boundary conditions (respectively PBC, HBC). We recall that in order to avoid frustration of (short or long range) AFM ordering, it is necessary and sufficient that the lengths L_1 and L_2 of the lattice be (i) both even for PBC and (ii) one even, the other odd, for HBC. We have incorporated this restriction in our work.

In Fig. 1 we show the comparison for the $h = 0$ case. We have found that for similar size lattices, the calculation with helical boundary conditions yields zeros that lie generally slightly closer to the limaçon than the calculation with periodic boundary conditions. Accordingly, we show in Fig. 1 the zeros for a 7×8 lattice with helical boundary conditions. In the vicinity of the FM-PM and PM-AFM critical points the density of zeros calculated on the finite lattice decreases as one approaches the real axis, in accord with the exact result [3,10] that in the thermodynamic limit this density g vanishes, in our notation, like $g(u, \mu = 1) \sim |(1-u/u_c)(1-uu_c)|^{1-\alpha}$ as $u \to u_c$ or $u \to 1/u_c$ along the curves of zeros, where $\alpha = \alpha'$ is the specific-heat exponent, for both of these critical points. As one approaches the singular point $u = -1$ from within the FM, AFM, or PM phases, the specific heat C has logarithmic divergences [5], i.e., $\alpha_s = \alpha'_s = 0$. Together with a generalization of the above relation for g, viz.,

$$g \sim |1 - u/u_{\rm sing}|^{1-\alpha'_{\rm sing}} \quad \text{as} \quad u \to u_{\rm sing} \tag{3.8}$$

along the curve(s) where g has nonzero support, this implies that $g(u, \mu = 1) \sim |1 + u| \to 0$ as $u \to -1$ along the curves of zeros comprising the complex-temperature phase boundaries. The behavior of the zeros in Fig. 1 is evidently consistent with this exact result. Indeed, one observes that the zeros avoid the region $u = -1$. A similar tendency of the zeros not only to become less dense but also to deviate from the limaçon can be seen in the vicinity of the PM-AFM critical point, where the last complex-conjugate pair of zeros occur significantly within the curve. (By the $u \to 1/u$ symmetry, this is equivalent to the inverse deviation of the last complex-conjugate pair of zeros near the FM-PM critical point.) The fact that there are no zeros on the positive real u axis is, of course, also implied by the property that for $H = 0$, the partition function for a finite lattice is a generalized polynomial in u with positive coefficients.

2. $\mu = -1$

We have performed a similar comparison for $\mu = -1$ and show a plot of the zeros in Fig. 2, again for a 7×8 lattice with helical boundary conditions [31]. One sees that

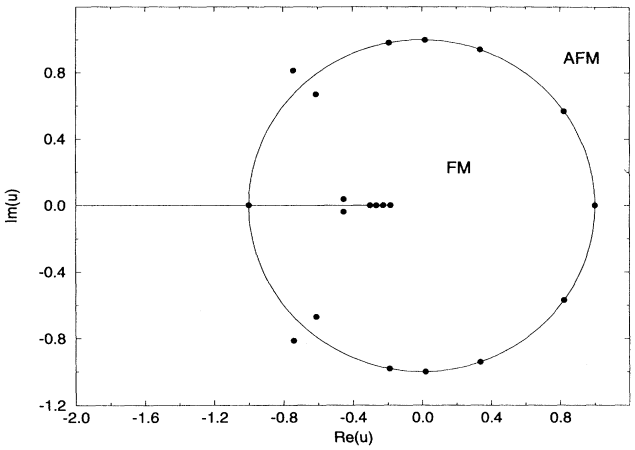

FIG. 2. Complex-temperature zeros of Z, calculated for $h = i\pi/2$ ($\mu = -1$) on a 7×8 lattice with helical boundary conditions, as compared with the exact result, in the $u = e^{-4K}$ plane.

all of the zeros in the right-hand half plane, and several other zeros, lie exactly (to within numerical accuracy) on the unit circle. The zero at $u = 1$ has multiplicity $N_s/2$ ($= 28$ here), consistent with the fact that in the thermodynamic limit, the (reduced) free energy f contains an additive term $(1/2)\ln(1-u)$ [see Ref. [6] and Eq. (2.29) of Ref. [32] corresponding to a δ function in the density of zeros, g, at $u = 1$. Because of this δ function singularity in g, the relation expressing the specific heat as an integral of g over the region where it has nonzero support receives an additive contribution. In turn, this has the effect of modifying the relation (3.8) connecting g with the critical exponent in the specific heat at a singular point $u_{\rm sing}$, hence, the fact, shown in Ref. [19], that the specific heat C has a finite nonanalyticity ($\alpha'_1 = 0$) at $u = 1$ as this point is approached from the FM or AFM phases does not conflict with the nonvanishing of g at $u = 1$. On the negative real axis, there are zeros lying on (or near) the line segment in (3.5). As one can see from Fig. 2, near the inner (and by the $u \to 1/u$ symmetry, also the outer) end point of the line segment, the density of zeros approaches a nonzero constant. This finite-lattice feature is in good agreement with the infinite-lattice relation (3.8) between g and the specific-heat singularity, together with the exact exponent that we found earlier [19], $\alpha'_e = 1$, at $u = u_e$ and $u = 1/u_e$. Proceeding next to the intersection point at $u = -1$, we observe that our exact result that the specific heat has a finite nonanalyticity ($\alpha'_s = 0$) at $u = -1$ as this point is approached from either the FM or AFM phase [19] implies that in the thermodynamic limit, $g(u, \mu = -1) \sim |1 + u| \to 0$ as one approaches this point along the unit circle or the negative real axis. This is consistent with the results in Fig. 2. (It happens that for the 7×8 lattice with HBC there is a zero precisely at $u = -1$, but this does not occur for other lattice sizes and is not a general feature.) Finally, we note a contrast with the $h = 0$ case: there,

Z was a generalized polynomial in u with positive coefficients, whereas here the coefficients are not all positive, so that zeros can, and indeed do, occur on the real u axis. One quantitative measure of how well the zeros on the finite lattices approach the locus of zeros on the infinite lattice is provided by how close the innermost zero on the negative Re(u) axis is to the infinite-lattice result, $u_e = -(3 - 2\sqrt{2})$. We find that the position of this zero is (i) $u = -0.1822$ on an 8×8 lattice with PBC, and (ii) $u = -0.1831$ on a 7×8 lattice with HBC. These points are, respectively, 6.2% and 6.5% farther away from the origin than u_e.

IV. COMPLEX-TEMPERATURE PROPERTIES FOR $0 < H \leq \infty$ $(0 \leq \mu < 1)$

A. Information from zeros of Z

Having these comparisons with exactly solvable cases as background, we now proceed to investigate the complex-temperature phase diagram and associated singularities for the Ising model in a nonzero magnetic field, i.e., $0 < H \leq \infty$, or equivalently, $0 \leq \mu < 1$. Since any nonzero magnetic field explicitly breaks the Z_2 symmetry of the Hamiltonian, the Z_2-symmetric, PM phase immediately disappears. We recall from Sec. (II B) that H can be taken positive without loss of generality, and that the results for the above interval in μ also describe the behavior for $1 < \mu \leq \infty$. Of the four symmetries in Sec. (II B), the $u \to 1/u$ symmetry of the phase diagram (with corresponding interchange of FM and AFM phases) ceases to hold if $\mu \neq \pm 1$. One may inquire how the complex-temperature phase boundary changes as H is increased from zero. One knows rigorously that for $h \neq 0$, it is possible to analytically continue from $u = 0$ out along the positive real u axis through the point u_c (which is no longer a critical point), all the way to the vicinity of $u = 1$ $(K = 0)$. This means that the region that was previously, for $H = 0$, the PM phase and its complex-temperature extension, immediately becomes part of the FM phase and its complex-temperature extension, respectively. This also means that for any nonzero h, the inner branch of the limaçon, which formed the phase boundary between the FM and PM phases for $H = 0$, breaks apart at $u = u_c$ into two separate arcs, leaving an opening through which the analytic continuation mentioned above can be performed.

One also knows that if $J < 0$, then for a fixed value of H, at sufficiently low T, the system will still exhibit long-range AFM ordering. Equivalently, for fixed h and hence μ, and sufficiently large $u > 1$ (i.e., sufficiently large negative K), there will be AFM ordering. Thus, for any finite h, there is still a nonanalytic boundary separating the physical and CT extension of the FM phase from the physical and CT extension of the AFM phase. Since the nonzero H biases the system toward FM ordering and hence against AFM ordering, it follows that the singular point that separates the physical FM and AFM phases, $u_{\rm FM,AFM}$, increases as H increases (starting from the value $\lim_{H\to 0} u_{\rm FM,AFM} = 1/u_c$). As u increases through the value $u_{\rm FM,AFM}$, the system undergoes a first-order transition at which M jumps discontinuously to zero. One expects that generic points on the border between the (complex-temperature) FM and AFM phases are also associated with a first-order phase transition. Given the biasing effect of nonzero H, one expects the complex extension of the FM phase to increase as H increases. Because of the symmetry under $h \to -h$ noted above, it follows that the rightward shift in $u_{\rm FM,AFM}$ as a function of H is independent of the sign of H. An additional general statement is that for all H (zero or not), the (complex-temperature extensions of the) FM and AFM phases must be completely separated by a phase boundary.

In Fig. 3 we show a combined plot of the CT zeros of Z, calculated for the same lattice (7×8 with helical boundary conditions) as before, for a sequence of increasing values of h, and in Fig. 4 we show plots of these zeros for certain fixed values of h. There are several interesting features that we can discern from these calculations. The results are in accord with the expectations based on rigorous arguments noted above. As h increases above zero (μ decreases below 1), the right-hand end of the inner branch of the limaçon, which formerly crossed the real u axis at u_c immediately breaks at $u = u_c$, rendering it possible to analytically continue from $u = 0$ along the positive real axis outward past $u = 0$ all the way to the vicinity of $1/u_c$. This breaking yields two complex-conjugate arcs, which retract from the real u axis as h increases. Scaling arguments imply that in the neighborhood of $h = 0$, the end point of the arc in the upper half plane should move in the direction [20]

$$\theta_{\rm ae} = \frac{\pi}{2\beta\delta}. \tag{4.1}$$

For the 2D Ising model, inserting the exactly known crit-

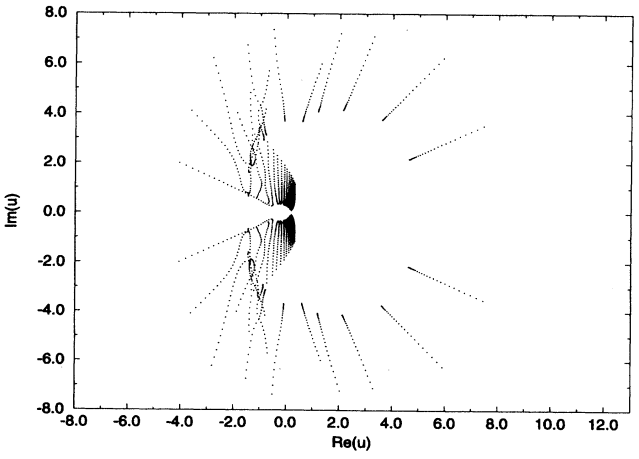

FIG. 3. Zeros of Z in the u plane, for h varying from 0 to 1.25 in increments of 0.05. Lattice size and boundary conditions are as in Fig. 1.

ical exponents $\beta = 1/8$ and $\delta = 15$, it follows that

$$\theta_{ae,2D} = \frac{4\pi}{15} = 48°. \tag{4.2}$$

One can see roughly, and we have confirmed accurately, that this is in agreement with the motion of the zero nearest to u_c for small h. The direction of motion away from the origin is different for the zeros on the inner arcs. Related to this, as h increases, the upper arc becomes oriented in a more northwest to southeast, rather than west to east, direction.

A notable feature that one sees in each of the graphs in Fig. 4 is that there is a sharp increase in the density of zeros as one approaches the end points of these arcs. This suggests the possibility that in the thermodynamic limit the density g might actually diverge as one approaches these end points along the arcs. Below, we shall find support for this conclusion from our analysis of low-temperature series, which yields a value for the specific-heat exponent $\alpha'_{ae} > 1$ at these end points; together with the relation (3.8), such a value of α'_{ae} implies that g diverges at the arc end points. Note also, of course, that $\alpha'_{ae} > 1$ also means that the internal energy diverges at these end points. In this context, we recall that in our study of the complex-temperature singularities of the Ising model on the honeycomb lattice [24], we found the exact result that at the point $z = -1 \equiv z_\ell$, as approached from either the FM or AFM phase, the specific heat diverges with an exponent $\alpha'_\ell = 2$.

In accord with the argument given above, as h increases, $u_{\rm FM,AFM}$ increases, and, more generally, one sees that in the right-hand half plane, the zeros on what was the outer branch of the limaçon for $h = 0$ move outward. The directions of motion of these zeros are approximately radially outward and do not change significantly as h is increased. Of course, the fact that the zeros on what were, for $h = 0$, the inner and outer branches of the limaçon both move outward is a striking manifestation of the loss of the $u \to 1/u$ symmetry, which held for $h = 0$, since the latter symmetry implied that these zeros were inverses of each other (so that if the inner branch moved out, the outer branch would have had to move in). From the comparison of the zeros calculated on finite lattices with the exact phase boundary for $H = 0$, we saw that the pair of zeros farthest to the right lies within the outer branch of the limaçon. One thus anticipates that this may also be true for nonzero H. Numerical estimates of $K_b = J/[k_B T_b(H)]$, expressed in terms of the

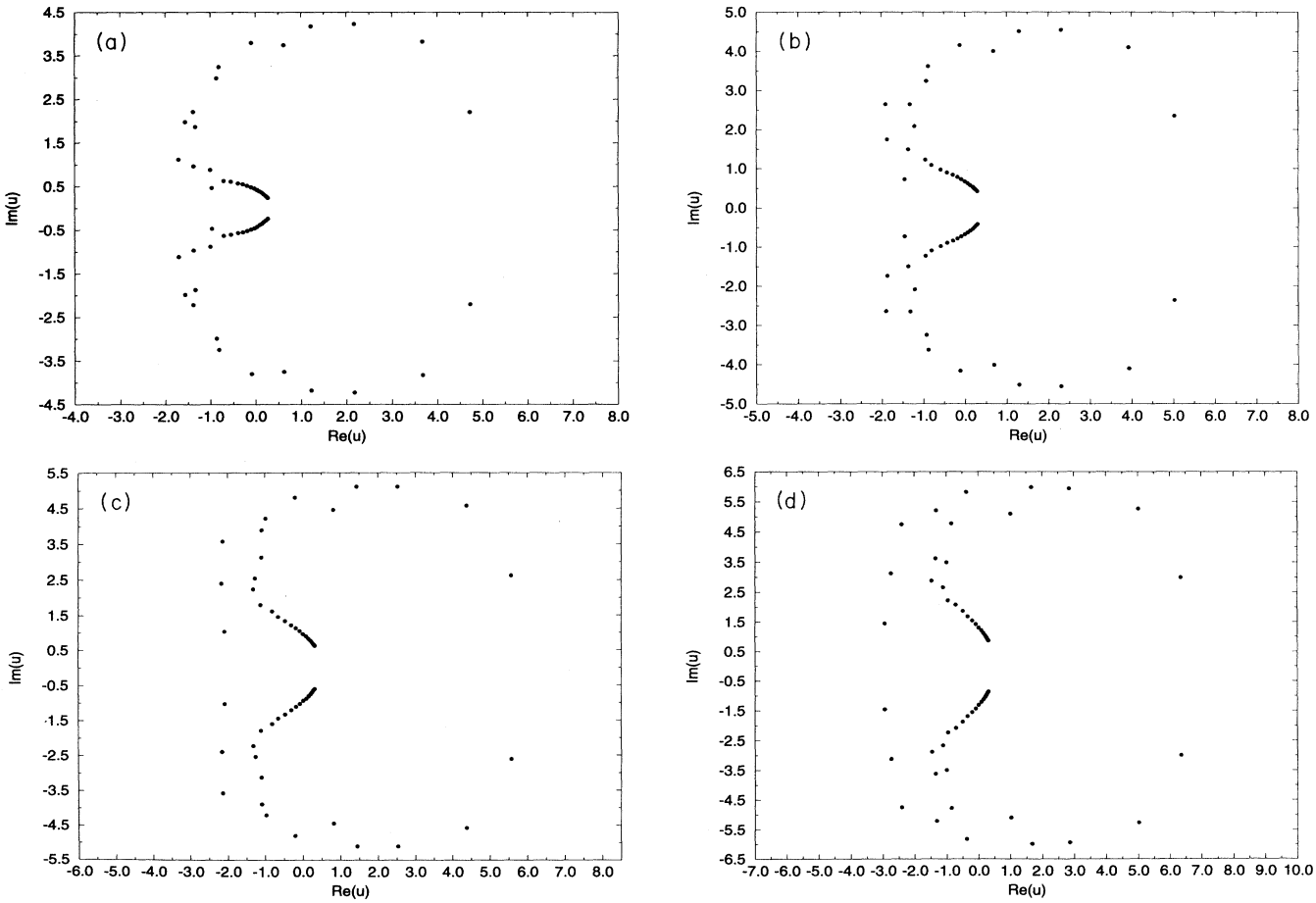

FIG. 4. Zeros of Z in the u plane, for h= (a) 0.25, (b) 0.5, (c) 0.75, and (d) 1.0. Lattice size and boundary conditions are as in Fig. 1.

u variable, are $u_{\rm FM,AFM} = 5.909\,09(9)$, $6.340\,36(9)$, and $7.993\,33(10)$ for $h = 0.2$, 0.5, and 1.0, respectively, where the number in brackets is the uncertainty in the last digit [9]. If we draw a curve through the zeros on the right-hand side of the phase diagram, and then compare the point at which they cross the real axis with these values, we see that, indeed, the finite lattice calculations yield a slight underestimate of this point for nonzero H, as they did for $H = 0$.

The motion of the zeros in the left-hand half plane is more complicated. One sees that, while the zeros do move generally outward from the origin as H increases, the directions of motion of a number of zeros undergo significant (and nonmonotonic) changes. We note that, owing to the loss of the inversion symmetry for $\mu \neq \pm 1$, the self-inverse point $u = -1$ loses the special significance that it had for these two values, for which it was an intersection point on the respective phase boundaries.

From these calculations, we may draw some further inferences about the phase diagram in the thermodynamic limit. As h increases, the boundary between the FM and AFM phases on the right-hand side of the phase diagram moves outward from the outer branch of the limaçon. On the left-hand side, the intersection point at $u = -1$ is replaced by an outer boundary to the left of this point, which shows some concavity but moves farther to the left as h increases. Recall that for $h = 0$, the inner and outer branches of the limaçon cross in a perpendicular manner at this point [5] (see Fig. 1). Our calculations suggest that it is likely that as h increases from 0, the curves which, for $h = 0$, were the inner and outer branches of the limaçon, no longer intersect at $u = -1$; instead, the upper and lower parts of the former outer branch join smoothly to each other on the left, and cross the real u axis in a vertical manner rather than as perpendicular NW-SE and SW-NE curves. Our results also suggest that the two complex-conjugate arcs which, for $h = 0$, comprised the connected inner branch of the limaçon, no longer cross the negative real u axis at $u = -1$ but instead retract from this axis. It is possible that they join the outer phase boundary (at complex-conjugate points). As h increases more, our calculated zeros indicate that these complex-conjugate arcs move progressively farther from the real axis. As $h \to \infty$, the boundary separarating the FM and AFM phases moves outward to complex infinity in the u plane, so that in this limit, the entire plane is occupied by the FM phase. We shall next obtain further information about the end points of these arcs from a series analysis.

B. Results from series analysis

In order to investigate the complex-temperature singularities for $-1 < \mu < 1$, we shall make use of the low-temperature, high-field series expansion for the free energy of the Ising model on the square lattice [26–28]. The partition function Z can be written as $Z = e^{N_s(2K+h)} Z_r$, and equivalently, the reduced free energy can be written as $f = 2K + h + f_r$, where $f_r = \lim_{N_s \to \infty} N_s^{-1} \ln Z_r$. In Ref. [28], Baxter and Enting calculated the low-temperature expansion of the quantity $\kappa = e^{f_r} = \lim_{N_s \to \infty} Z_r^{1/N_s}$ to $O(u^{23})$ (with the coefficients of the powers of u being exact polynomials in μ). This expansion has the form

$$\kappa = 1 + \sum_{n=2}^{\infty} \sum_{m} a_{n,m} u^n \mu^m, \tag{4.3}$$

where $j \le m \le j^2$ for $n = 2j$ and $j \le m \le j(j-1)$ for $n = 2j - 1$. From this series, we calculate, for each value of μ, resultant series for the specific heat C, magnetization M, and susceptibility $\bar{\chi}$. We then analyze these using $d$log Padé and differential approximants (abbreviated PA and DA; for a recent review, see [29]). Our notation for differential approximants follows that in Ref. [29] and our implementation is the same as that in Ref. [19]; in particular, we use unbiased, first-order differential approximants.

We find from both the PA and DA analysis that for $0 < \mu < 1$, the series indicate a complex-conjugate pair of singularities at positions that are in very good agreement with the locations of the innermost zeros on the inner arcs. We denote these arc end points, $u_{\rm ae}$ and $u_{\rm ae}^*$. Table I shows the comparison of the values of the arc end point u_{ae} as obtained from the complex-temperature zeros on finite lattices and from the analysis of the low-temperature series. The fractional differences in the positions are about 2%.

We have made a preliminary study of the singularities at these arc end points. Since the arc end points arise abruptly with the breaking of the inner branch of the limaçon for any h, regardless of how small, one antici-

TABLE I. Values of the arc end point, $u_{\rm ae}$, for several values of h, from (i) calculation of zeros of Z on finite lattices, yielding $u_{\rm ae,Z}$, and (ii) analyses of series for C, M, and $\bar{\chi}$, yielding $u_{\rm ae,ser}$. Values of the exponents $\alpha'_{\rm ae}$, $\beta_{\rm ae}$, and $\gamma'_{\rm ae}$ at $u_{\rm ae}$ as determined from analysis of low-temperature series using $d$log Padé and differential approximants are also given. The values of $u_{\rm ae,ser}$ are quoted to an accuracy in accord with the agreement between the different series and methods of analysis. The values for $u_{\rm ae,Z}$ are quoted to an accuracy reflecting the differences in values with different boundary conditions. The numbers in parentheses denote the uncertainties in the last digit of a given entry.

h	μ	$u_{\rm ae,Z}$	$u_{\rm ae,ser}$	$\alpha'_{\rm ae}$	$\beta_{\rm ae}$	$\gamma'_{\rm ae}$
0.8	0.202	$0.313 + 0.663i$	$0.3203(6) + 0.6503(6)i$	1.175(7)	−0.18(5)	1.195(10)
1.0	0.135	$0.320 + 0.857i$	$0.3265(5) + 0.8426(6)i$	1.177(8)	−0.18(5)	1.20(2)
1.2	0.0907	$0.324 + 1.086i$	$0.3306(5) + 1.0685(6)i$	1.18(2)	−0.18(5)	1.19(2)

pates a similarly abrupt change in exponents. Indeed, in our previous studies of complex-temperature singularities (e.g., Refs. [23, 24]), using exact results, we found that M always diverges at end points of arcs protruding into the FM phase. Hence, we expect (and will verify) that M diverges at the arc end points in the present case, so that β jumps discontinuously from the value $\beta = 1/8$ for $h = 0$ to negative value(s) for nonzero h. We assume the usual leading singular forms

$$C \sim A_C(1 - u/u_{\rm ae})^{-\alpha'_{\rm ae}}, \tag{4.4}$$

$$M \sim A_M(1 - u/u_{\rm ae})^{\beta_{\rm ae}}, \tag{4.5}$$

$$\bar{\chi} \sim A_\chi(1 - u/u_{\rm ae})^{-\gamma'_{\rm ae}}. \tag{4.6}$$

(We do not consider confluent singularities here; at least for $H = 0$, they are unimportant for the 2D Ising model, a fact used also in our previous study of complex-temperature singularities in this case [5].) We analyze the singularities for three values of h that are chosen to be sufficiently large that the arc end points are reasonably well separated from each other, viz., $h = 0.8$, 1.0, and 1.2. We obtain the results shown in Table I. In the case of $\alpha'_{\rm ae}$ and $\gamma'_{\rm ae}$, the $d\log$ Padé and differential approximants yielded values in very good agreement with each other. In the case of $\beta_{\rm ae}$, the PA's gave somewhat larger values than the DA's; we list values that are more heavily weighted by the (presumably more accurate) DA's, with estimated errors that are increased to reflect the PA results. As is evident from Table I, for the values of h that we have considered, these exponents are consistent with being independent of the value of h in this range. The values of the exponents are also consistent with the equality $\alpha'_{\rm ae} + 2\beta_{\rm ae} + \gamma'_{\rm ae} = 2$. The fact that $\beta_{\rm ae}$ is negative means that M diverges at the arc end points; this is the same behavior that we found earlier in our studies of complex-temperature singularities on various lattices, using the respective exact expressions for the magnetization (e.g., see the summary in Table II of Ref. [23]). Our results also indicate that $\alpha'_{\rm ae} > 1$. As noted above, in conjunction with the relation (3.8), this implies that in the thermodynamic limit the density g of zeros of Z diverges as one moves along the arcs and approaches their end points. The behavior of the zeros calculated on finite lattices already suggests this infinite-lattice result.

V. PHASE DIAGRAM FOR $-1 \le \mu \le 0$

A. Zeros of Z

This range of μ is not physical, in contrast to the range $0 \le \mu \le 1$ discussed above. Nevertheless, it is of interest because by determining how the phase diagram changes as μ decreases through this range, we can complete the connection between the exact solutions at $\mu = 1$ and -1.

For the discussion of the complex-temperature zeros of Z, just as in the previous section, we started with the exactly known case $\mu = 1$ and moved away from it by decreasing μ, so it is also convenient here to start with the exactly known phase diagram for $\mu = -1$ and move away from it by decreasing the magnitude of μ toward 0. In Fig. 5 we show a plot of the paths of individual zeros for a sequence of values of h, and in Fig. 6 we show plots of zeros for fixed values of h. These results have a number of salient features. First, as μ moves from -1 toward 0^-, the zeros that were on the unit circle move approximately radially outward to larger values of $|u|$. They maintain a roughly circular form. The zeros that had been on or close to the negative real axis and had corresponded to what, in the thermodynamic limit, was the line segment in (3.5) extending between $1/u_e$ and u_e for $\mu = -1$, move gradually outward, away from the origin. Meanwhile, for any value of μ greater than -1, there abruptly appears a new set of zeros on the positive real axis. Our calculations of zeros on finite lattices suggest the inference that in the thermodynamic limit, these form a finite line segment of singular points starting initially at $u = 1$ for $\mu = -1 + \epsilon$, $\epsilon \to 0$ (and extending rightward). As μ increases from -1 (again in the thermodynamic limit), the right-hand phase boundary between the FM and AFM phases moves outward sufficiently quickly that, as one can see in Fig. 6, it lies to the right of the new line segment of zeros on the positive real u axis (presumably connecting with the right-hand end point of this line segment). We shall denote the respective end points, in the thermodynamic limit, of the left-hand and right-hand line segments of zeros as $u_{\rm lhe}$ and $u_{\rm rhe}$. A striking feature of the plots is that the density of zeros increases sharply as one moves rightward toward the inner end of the line segment of zeros on the negative real u axis, and also as one moves leftward toward the inner end of the line segment of zeros on the positive real axis. This is quite similar to what we observed for the density of zeros near the arc end points in the FM phase for $0 \le \mu < 1$. Again, it suggests the inference that in the infinite-lattice limit, the density of zeros g diverges at these end points $u_{\rm lhe}$ and $u_{\rm rhe}$. Our series analysis below supports this inference. The results in Fig. 6 also show that as μ moves toward 0

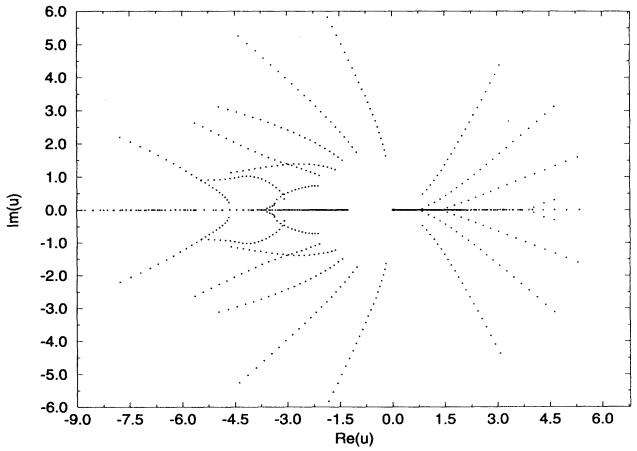

FIG. 5. Zeros of Z in the u plane for $-1 < \mu < 0$. Denoting $h = i\pi/2 + h_r$, h_r varies from 0.25 to 1.25 in increments of 0.05. Lattice size and boundary conditions are as in Fig. 1.

through the interval $-1 < \mu < 0$, the end points of the line segments, $u_{\rm lhe}$ and $u_{\rm rhe}$ move slowly away from the origin. As $\mu \to 0^-$, the boundary separating the FM and AFM phases moves outward to complex infinity, so that in this limit, only the FM phase remains. This can be understood on general grounds, as we have discussed above.

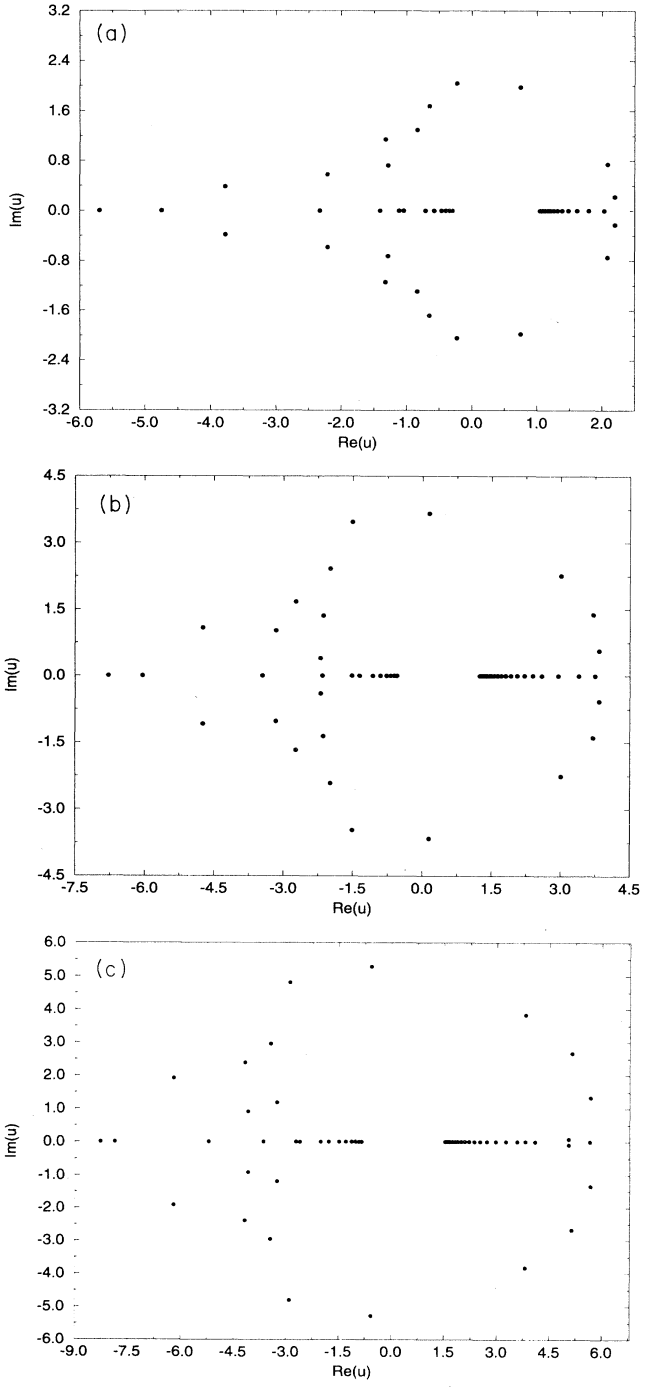

FIG. 6. Zeros of Z in the u plane for μ= (a) -0.5, (b) -0.2, (c) -0.1. Lattice size and boundary conditions are as in Fig. 1.

B. Series analysis

From our analysis of the low-temperature series for C, M, and $\bar{\chi}$, we have obtained very good agreement with the positions of the inner end points of the left and right line segments, $u_{\rm lhe}$ and $u_{\rm rhe}$. Table II displays this comparison. Of course, one cannot use the series to locate the outer end point of the left line segment, since it lies outside the FM phase where these series are applicable. We have also found that one cannot use the series to locate the outer end point of the right line segment; as in our earlier work [24], the reason is that this end point is shielded from the origin by the intervening right-hand line segment of singularities, and the series are dominated by the singularitities at the inner end points of the two line segments. Since

$$\lim_{\mu \to -1} u_{\rm lhe} = u_e \tag{5.1}$$

and since the exponents are known for $\mu = -1$ as [19] $\alpha'_e = 1$, $\beta_e = -1/8$ (exact), and $\gamma'_e = 5/4$ (inferred from series analysis), an interesting question is whether, for values of μ in the interval $-1 < \mu < 0$, the singularities in C, M, and $\bar{\chi}$ at the inner end point of the left line segment are described by exponents that are (i) independent of μ in this interval, and (ii) equal to their values at $\mu = -1$. In Table III we list our results for $\mu = -0.5$ and -0.2 (the results for $\mu = -0.1$ were less precise). The values for $\alpha'_{\rm lhe}$ and $\gamma'_{\rm lhe}$ from the d log Padé and differential approximants agreed very well with each other. The value of $\beta_{\rm lhe}$ was more difficult to extract from the series analysis (in particular, the d log Padé approximants yield somewhat larger values than the differential approximants); using only the (presumably more accurate) DA's, we obtain the value given in Table III. To within the estimated uncertainties, these results are consistent with being independent of μ for the two values of μ considered, and with satisfying the equality $\alpha'_{\rm lhe} + 2\beta_{\rm lhe} + \gamma_{\rm lhe} = 2$. Regarding question (ii), $\gamma'_{\rm lhe}$ is slightly, but not decisively, lower than the inferred value at $\mu = -1$, $\gamma'_e = 5/4$. The exponent $\beta_{\rm lhe}$ is also consistent with the $\mu = -1$ value, $\beta_e = -1/8$, but the large uncertainty in its determination precludes a sensitive test of this equality. The values of $\alpha'_{\rm lhe}$ are about 4σ above unity. Assuming the series analysis gives a re-

TABLE II. Values of the inner end points of the left and right line segments for negative μ, with $h = -(1/2)\ln\mu = h_r + i\pi/2$. Entries in the columns denoted $u_{\rm lhe,Z}$ and $u_{\rm rhe,Z}$ are the innermost zeros on the left- and right-hand line segments, calculated on a 7×8 lattice with helical boundary conditions. Entries in the columns denoted $u_{\rm lhe,ser}$ and $u_{\rm rhe,ser}$ are the positions of the inner end points of the left and right line segments as obtained from the analyses of low-temperature series for C, M, and $\bar{\chi}$. Accuracies listed are chosen as in Table I.

h_r	μ	$u_{\rm lhe,Z}$	$u_{\rm lhe,ser}$	$u_{\rm rhe,Z}$	$u_{\rm rhe,ser}$
0.347	-0.5	-0.2976	$-0.2870(5)$	1.047	1.053(15)
0.805	-0.2	-0.5467	$-0.5314(8)$	1.246	1.245(10)
1.151	-0.1	-0.8471	$-0.8267(8)$	1.529	1.522(10)

TABLE III. Values of the singular exponents $\alpha'_{\rm lhe}$, $\beta_{\rm lhe}$, $\gamma'_{\rm lhe}$, α'_{rhe}, $\beta_{\rm rhe}$, and $\gamma'_{\rm rhe}$ at the inner end points of the left- and right-hand line segments, $u_{\rm lhe}$ and $u_{\rm rhe}$, respectively, as determined from analyses of low-temperature series for C, M, and $\bar{\chi}$ using $d\log$ Padé and differential approximants.

μ	$\alpha'_{\rm lhe}$	$\beta_{\rm lhe}$	$\gamma'_{\rm lhe}$	$\alpha'_{\rm rhe}$	$\beta_{\rm rhe}$	$\gamma'_{\rm rhe}$
-0.5	1.20(5)	$-0.2(1)$	1.20(4)	1.65(12)	$-0.35(20)$	1.00(15)
-0.2	1.18(5)	$-0.2(1)$	1.19(5)	1.4(1)	$-0.2(1)$	1.15(20)

liable determination of this exponent, this means that it is not equal to the $\mu = -1$ value, $\alpha'_e = 1$. Furthermore, it means that the density of zeros does diverge at $u_{\rm lhe}$, a conclusion already hinted at by the behavior of the zeros calculated on finite lattices.

We have also extracted the critical exponents at the inner end point of the right-hand line segment $u_{\rm rhe}$ from series analysis. Here there are two specific questions to investigate. First, are these exponents consistent with being independent of μ in the range $-1 < \mu < 0$? Second, recalling that, in the limit $\mu \to -1$, the right line segment decreases in length and eventually disappears at $u = 1$ (as inferred from our finite-lattice calculations, in agreement with our series analysis), one would like to see whether the exponents on the inner end point of this right-hand line segment, $u_{\rm rhe}$, might be equal to those that we found for the singularity at $u = 1$ for $\mu = -1$, viz., $\alpha'_1 = 0$ (finite logarithmic nonanalyticity in C), $\beta_1 = -1/4$ (both exact), and $\gamma'_1 = 5/2$ (inferred from series analysis) [19]. Our results are shown in Table III. Just as was true of the inner end point of the left line segment, it was more difficult to get an accurate value of $\beta_{\rm rhe}$, and again we have quoted a value weighted more by the differential approximants, with a commensurately large uncertainty assigned. These values of critical exponents at the inner end point of the right-hand line segment are crudely consistent, to within large uncertainties, with being independent of μ over the indicated range of μ. They are also in accord with the hypothesis that $\alpha'_{\rm rhe} + 2\beta_{\rm rhe} + \gamma'_{\rm rhe} = 2$. As $\mu \to -1$, we find that it is more difficult to get accurate values for the singular exponents. This is not surprising, since in this limit the right line segment disappears. Regarding the second question, although the uncertainties in the critical exponents are large, our results indicate that, for the range of μ considered, the exponents $\alpha'_{\rm rhe}$ and $\gamma'_{\rm rhe}$ are not equal to the respective exponents at $u = 1$, $\mu = -1$. We cannot draw a firm conclusion concerning whether over the same range of μ, $\beta_{\rm rhe}$ is equal to or unequal to β_1. The value(s) of $\alpha'_{\rm rhe}$ is about $(4\text{–}5)\sigma$ above 1, which supports the conclusion that the exact value of this exponent is, indeed, > 1, and hence that the density g of zeros diverges at $u_{\rm rhe}$, as it does at $u_{\rm lhe}$. This is again consistent with the observed behavior of the zeros calculated on finite lattices.

VI. COMMENTS ON OTHER LATTICES

A. Honeycomb lattice

The complex-temperature phase diagram of the zero-field Ising model on a honeycomb lattice was determined in Ref. [24] from exact results. In the complex z plane the boundaries consist of the union of an arc of the unit circle $z = e^{i\theta}$, for $\pi/3 \le \theta \le 5\pi/3$ with a closed curve lying in the region $\mathrm{Re}(z) \ge 0$, which intersects the circle at $z = \pm i$ and the positive real z axis at z_c and $1/z_c$, where $z_c = 2 - \sqrt{3}$. This phase diagram consists of three complex-temperature phases: (i) FM, surrounding the origin, (ii) PM around $z = 1$, and (iii) AFM, the outermost phase, extending to complex infinity. The complex-temperature singularities were determined exactly for the specific heat and magnetization, and were studied using low-temperature series expansions for the susceptibility [24].

Here we determine the complex-temperature phase diagram for the honeycomb lattice at $\mu = -1$. One first uses the identity $e^{i(\pi/2)\sigma_n} = i\sigma_n$ to relate the model to one with no magnetic field and the partition function

$$Z = i^{N_s} \sum_{\sigma_n} \left(\prod_n \sigma_n \right) e^{\sum_{\langle nn' \rangle} \sigma_n K_{nn'} \sigma_{n'}} \tag{6.1}$$

(where we have allowed the possibility that the K_j along the three different lattice vectors are different). One can next associate dimers with pairs of σ's at neighboring sites and then reexponentiate these to express the partition function in terms of a model with the associated coupling K_j shifted by $i\pi/2$ [17, 18]. A complete dimer covering is provided by placing these dimers along one of the three lattice vectors on the honeycomb lattice. The situation is particularly simple, for the following reason: given that the coordinaton number is odd ($q = 3$), one can multiply by $1 = \sigma^2$ at each vertex and thereby place the dimers on every bond of the lattice, carry out the reexponentiation, and thus map the model to one with the couplings along each of the three lattice vectors shifted as $K_j \to K_j + i\pi/2$, $j = 1, 2, 3$. Since the shift is the same for each of these lattice directions, one can immediately specialize to the case of isotropic couplings. As a result, the reduced free energy f for $h = i\pi/2$ is given, up to an additive term $i\pi/4$, simply by that for $h = 0$ with the replacement $K \to K + i\pi/2$, or equivalently, $z \to -z$ or $v \to 1/v$. This is also true of C, M, M_{st}, and $\bar{\chi}$. Hence, we can directly take over our results for the zero-field case, and we find the complex-temperature phase diagram shown in Fig. 7. This consists of the FM, and AFM phases together with a phase in which $M = M_{st} = 0$ identically, whence the label ZM (standing for "zero uniform and staggered magnetization"). The magnetization satisfies $M(z, h = i\pi/2) = M(-z, h = 0)$, and similarly for the staggered magnetization. The points in the ZM phase are in 1:1 correspondence, under $z \to -z$, with the points in the PM phase of the zero-field model. The

reason that we do not label it as PM is that the nonzero magnetic field explicitly breaks the Z_2 symmetry, so that there is no PM phase in the strict sense. However, as discussed in Ref. [19], this noninvariance is manifested only in the noninvariance of the constant $i\pi/4$ in f, and hence does not affect derivatives such as C, M, and $\bar{\chi}$. We note the contrast with the square lattice, where for $\mu = -1$ (and indeed, also for all $\mu \neq 1$), there is no phase in which M and M_{st} both vanish; instead of becoming the ZM phase, the PM phase disappears completely. Our determination of complex-temperature singularities in $\bar{\chi}$ in Ref. [24] can also be taken over directly to the present case, with just the change $z \to -z$. The phase diagram in v shows the interesting feature that the FM and AFM phases are separated by a line of singular points on the imaginary v axis. This is similar to what we found for the square lattice [see Fig. 2(b) of Ref. [19]]. (A difference is that in the case of the square lattice, the FM and AFM phases extend to complex infinity in the right and left parts of the v plane, and hence the line separating them is the complete imaginary v axis, whereas for the honeycomb lattice, the FM and AFM phases are bounded by an oval-like curve [Fig. 7(b)] outside of which is the ZM phase, and the line segment separating them is finite, extending from $-i\sqrt{3}$ to $i\sqrt{3}$.)

As h increases from 0, the rigorous argument that one can analytically continue outward from $z = 0$ past the former FM-PM critical point at z_c, to the vicinity of the former PM-AFM critical point at $1/z_c$ implies, as in the case of the square lattice, that the right-hand boundary of the FM phase breaks open at $z = z_c$, forming two complex-conjugate arcs that retract away from the real axis. The former PM phase becomes part of the enlarged FM phase, again as in the square lattice case. The FM phase is completely separated from the AFM phase, and the former second-order critical point at $1/z_c$ which separated the PM and AFM phases for $h = 0$ now becomes a first-order phase boundary between the FM and AFM phases. The general arguments given above imply that as $\mu \to 0^+$ (and also for $\mu \to 0^-$), the FM phase expands to fill the entire z plane. Finally, for the special value $\mu = -1$, the model again exhibits a phase with $M = M_{st} = 0$, the ZM phase.

It may be noted that the simple relation under $z \to -z$ between the free energy and other thermodynamic functions that holds for this lattice also holds for heteropolygonal lattices with odd coordination number. Hence the complex-temperature phase diagrams for the 3×12^2 and 4×8^2 lattices with $h = i\pi/2$ are simply given by the diagrams that we worked out for the zero-field case [23] with the replacement $z \to -z$ (and PM $\to$ ZM).

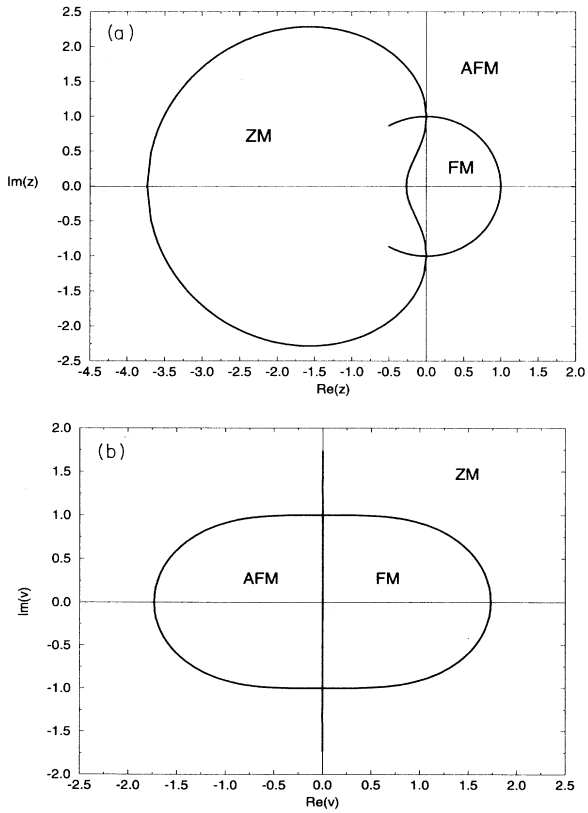

FIG. 7. Complex-temperature phase diagram for the Ising model on the honeycomb lattice with $\mu = -1$ in the variable (a) z, (b) v.

B. Triangular lattice

We recall that for the zero-field Ising model on the triangular lattice, the locus of complex-temperature points where the free energy is nonanalytic consists of the union of the circle

$$u = -\frac{1}{3} + \frac{2}{3}e^{i\theta} \tag{6.2}$$

(with $0 \le \theta < 2\pi$) and the semi-infinite line segment

$$-\infty \le u \le -\frac{1}{3}. \tag{6.3}$$

The FM phase is located within the circle, with the PM phase lying outside and extending to complex infinity.

By methods similar to those we have discussed, we calculate the complex-temperature phase diagram for $h = i\pi/2$ and show it in Fig. 8. In the u plane, the continuous locus of points where the free energy is nonanalytic consists of the union of the circular arc

$$u = \frac{1}{2}(-1 + e^{i\theta}) \ , \quad \theta_{ce} \le |\theta| \le \pi, \tag{6.4}$$

where

$$\theta_{ce} = \arctan\left(\frac{4\sqrt{2}}{7}\right) \simeq 38.9^\circ \tag{6.5}$$

corresponding to the end points $u_{ce} = e^{i\theta_{ce}}$ and u_{ce}^*, where

$$u_{ce} = \frac{-1 + 2^{3/2}i}{9} \tag{6.6}$$

and the semi-infinite line segment

$$-\infty \le u \le -\frac{1}{2}. \tag{6.7}$$

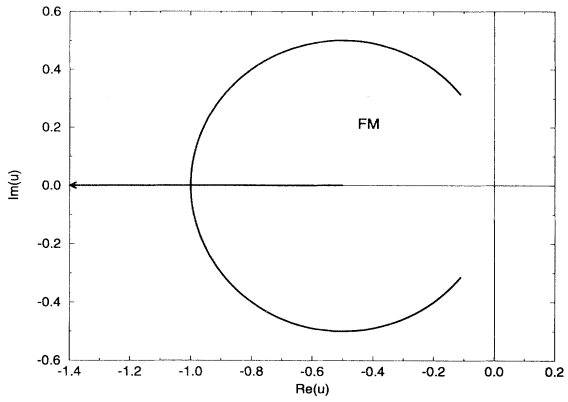

FIG. 8. Complex-temperature phase diagram for the Ising model on the triangular lattice with $\mu = -1$ in the variable u.

Just as there was no AFM phase for $h = 0$, so also there is none for $h = i\pi/2$. As h increases from 0, the PM phase abruptly disappears. By the same rigorous arguments as were discussed before, the right-hand boundary of the FM phase breaks open at $u = u_c = 1/3$ and the circle changes into a circular arc, the complex-conjugate end points of which retract away from the positive real axis. All points in the u (equivalently, z or v) plane (not lying on the above continuous locus of points where f is nonanalytic) are analytically connected to each other and all lie in the FM phase. The corresponding locus of points in the v plane consists of the union of a circular arc $v = e^{i\phi}$ traced out for $\phi_{ce} < \phi \leq \pi$, where $\phi_{ce} = \arctan(2^{3/2}/3) = 43.3°$ with two complex-conjugate arcs intersecting this circle at $v = \pm i$. Comparing the $h = 0$ and $h = i\pi/2$ complex-temperature phase diagrams in the u plane, one sees that the former circle of radius $2/3$ centered at $u = -1/3$ is replaced by an arc of a circle of radius $1/2$ centered at $u = -1/2$, and the semi-infinite line segment extending leftward from $u = -1/3$ is replaced by a similar line segment starting at $-1/2$.

VII. CONCLUSIONS

In this paper we have determined the general features of the complex-temperature phase diagram for the square-lattice Ising model in a nonzero external magnetic field $0 < h \leq \infty$ $(0 \leq \mu < 1)$. Our methods included calculations of complex-temperature zeros of the partition function for finite lattices and analysis of low-temperature series. We have also performed a similar analysis for $-1 < \mu \leq 0$. The results enable one to exhibit a continuous connection, via the variation of μ through real values from 1 to -1, of the two known exact solutions of this model, viz., those of Onsager and of Lee and Yang. We have studied the exponents in the specific heat, magnetization, and susceptibility at certain complex-temperature singularities that are present in the interval $-1 < \mu < 1$. Extending our earlier work, we have also determined the exact complex-temperature phase diagrams of the model at $\mu = -1$ on the honeycomb and triangular lattices and have discussed the relation between these and the zero-field phase diagrams. Our results give further information about the still-intriguing issue of the Ising model in a magnetic field.

This research was supported in part by the NSF Grant No. PHY-93-09888.

ACKNOWLEDGMENT

This research was supported in part by the NSF Grant No. PHY-93-09888.

[1] L. Onsager, Phys. Rev. **65**, 117 (1944).
[2] C. N. Yang, Phys. Rev. **85**, 808 (1952).
[3] M. E. Fisher, *Lectures in Theoretical Physics* (University of Colorado Press, Boulder, 1965), Vol. 7C, p. 1.
[4] S. Katsura, Prog. Theor. Phys. **38**, 1415 (1967).
[5] V. Matveev and R. Shrock, J. Phys. A **28**, 1557 (1995).
[6] T. D. Lee and C. N. Yang, Phys. Rev. **87**, 410 (1952).
[7] C. N. Yang and T. D. Lee, Phys. Rev. **87**, 404 (1952).
[8] J. L. Lebowitz and O. Penrose, Commun. Math. Phys. **11**, 99 (1968).
[9] H. W. Blöte and M. den Nijs, Phys. Rev. B **37**, 1766 (1988).
[10] R. Abe, Prog. Theor. Phys. **38**, 322 (1967).
[11] S. Ono, Y. Karaki, M. Suzuki, and C. Kawabata, J. Phys. Soc. Jpn. **25**, 54 (1968)
[12] C. J. Thompson, A. J. Guttmann, and B. W. Ninham J. Phys. C **2**, 1889 (1969); A. J. Guttmann *ibid.* **2**, 1900 (1969).
[13] C. Domb and A. J. Guttmann, J. Phys. C **3**, 1652 (1970).
[14] Y. Abe and S. Katsura, Prog. Theor. Phys. **43**, 1402 (1970).
[15] G. Marchesini and R. Shrock, Nucl. Phys. B **318**, 541 (1989); V. Matveev and R. Shrock, J. Phys. A **28**, L533 (1995); Phys. Lett. A **204**, 353 (1995).
[16] I. G. Enting, A. J. Guttmann, and I. Jensen, J. Phys. A **27**, 6963 (1994).
[17] D. Merlini, Lett. Nuovo Cimento **9**, 100 (1974).
[18] K. Y. Lin and F. Y. Wu, Int. J. Mod. Phys. B **4**, 471 (1988).
[19] V. Matveev and R. Shrock, J. Phys. A **28**, 4859 (1995).
[20] C. Itzykson, R. Pearson, and J. B. Zuber, Nucl. Phys. B **220**, 415 (1983).
[21] M. E. Fisher, Proc. R. Soc. London Ser. A **254**, 66 (1960); **256**, 502 (1966).
[22] W. van Saarloos and D. Kurtze, J. Phys. A **17**, 1301 (1984); J. Stephenson and R. Couzens, Physica (Amsterdam) **129A**, 201 (1984); D. Wood, J. Phys. A **18**, L481 (1985); J. Stephenson and J. van Aalst, Physica (Amsterdam) **136A**, 160 (1986).
[23] V. Matveev and R. Shrock, J. Phys. A **28**, 5235 (1995).
[24] V. Matveev and R. Shrock, J. Phys. A (to be published).
[25] K. Binder, Physica **62**, 508 (1972); T. de Neef and I. G.

Enting, J. Phys. A **10**, 801 (1977); I. G. Enting, Aust. J. Phys. **31**, 515 (1978); G. Bhanot, J. Stat. Phys. **60**, 55 (1990).

[26] M. F. Sykes, D. S. Gaunt, J. L. Martin, S. R. Mattingly, and J. W. Essam, J. Math. Phys. A **14**, 1071 (1973).

[27] M. F. Sykes, M. G. Watts, and D. S. Gaunt, J. Math. Phys. A **8**, 1448 (1975).

[28] R. J. Baxter and I. G. Enting, J. Stat. Phys. **21**, 103 (1979).

[29] A. J. Guttmann, in *Phase Transitions and Critical Phenomena*, edited by C. Domb and J. Lebowitz (Academic, New York, 1989), Vol. 13.

[30] Parenthetically, we note that for anisotropic spin-spin couplings, the complex-temperature zeros would merge to form areas instead of curves in the thermodynamic limit [22]. Indeed, for the (heteropolygonal) 4×8^2 lattice, even if the couplings are isotropic, the zeros still form areas in this limit [23].

[31] To save space, we truncate the plot on the left at $\mathrm{Re}(u) = -2$; there are four zeros lying on the negative real axis, and a pair lying near this axis, to the left of this point, which are not shown. However, the plot as shown contains all the information, since these six zeros are just the inverses, by the $u \to 1/u$ symmetry, of the six which are shown, lying on or near the negative real axis within the unit circle.

[32] As discussed in Ref. [19], in addition to this additive term there is also a subdominant contribution to the singularity in f at $u = 1$ arising from the vanishing of the argument of the logarithm in Eq. (2.29) of that paper.